11B.3 ADAPTIVE TECHNIQUE TO EXTRACT INTRINSIC INSECTS' BACKSCATTER DIFFERENTIAL PHASE FROM POLARIMETRIC SPECTRA

Svetlana Bachmann* and Dusan Zrnic
Cooperative Institute for Mesoscale Meteorological Studies, University of Oklahoma and
NOAA/OAR National Severe Storm Laboratory, Norman, Oklahoma

1. INTRODUCTION

Radar echoes from optically clear air are weak. Such echoes may be enhanced by weakly flying insects or/and contaminated by actively flying insects and birds. Both birds and insects are present in great numbers over the Great Plains in the United States. Both the types and the numbers of insects and birds exhibit seasonal changes and diurnal-nocturnal fluctuations. Often, birds and insects share airspace resulting in radar detection of echoes from the bird-insect-mix. The signatures of birds can be identified and filtered from such bird-insect-mix and the remaining signatures of insects can be used to evaluate properties of the wind, keeping in mind that insects might not be wind-blown and could introduce a small bias to the velocity estimates. In term of polarimetric spectral signatures, insects' contributions to the echoes often result in larger values of differential reflectivity, smoother fields of backscatter differential phase, and larger values of co-polar correlation coefficient compared to the contributions from birds. Because of these properties, insects' signatures can be extracted from spectra and studied.

We examine the change in polarimetric variables of biological scatterers over one evening. We apply a special technique on the polarimetric spectral densities for estimating the backscatter differential phase δ inherent to insects. The field of δ obtained with our method is smoother compared to the field of δ obtained by standard procedures. Nonetheless, the values in the east and west semicircles of radar coverage defy simple explanation. It might be that the body shapes of the ascending/descending insects are responsible for the non symmetric signature of δ field. It is possible that the nocturnal insects are emerging on the east side while the diurnal insects are still present and descending on the west side during the dusk. The changes are rapid so that the observations at the time intervals shorter than 10 minutes are needed to capture the continuity of the evolution during sunset. Even after the sunset the biological inhabitants of the atmosphere present evolving and somewhat inhomogeneous fields of polarimetric variables. We use presented technique to study the signatures of insects. The technique might be useful for discriminating different types of insects and is definitely suited for separating insects from birds.

* *Corresponding author address*: Svetlana Bachmann, CIMMS, 120 David L. Boren Blvd., Norman, OK 73072, USA; e-mail: svetlana.bachmann@noaa.gov

Adaptive selection in the frequency domain allows us to suppress signatures of migrating birds or other scatterers and to extract signatures of insects that can be characterized by high differential reflectivity and co-polar correlation coefficient.

2. DATA COLLECTION AND ANALYSES

Time-series data were collected with the research 10 cm wavelength polarimetric radar (KOUN) in Norman, OK, USA. KOUN is maintained and operated by the National Oceanic and Atmospheric Administration / National Severe Storm Laboratory (NOAA/NSSL). Data case includes 13 data sets collected with the unevenly spaced time intervals on September 7, 2004 between 6 pm and 11 pm local time (2300 and 0400 UTC). We use local time notation for natural association of the progression of the evening with the observed changes. Optically clear air, a light N-NW wind, and migrating birds were reported on this evening. The sunset was at 7:57 pm. Radar was in dual-polarization mode, transmitting and receiving simultaneously waves of horizontal and orthogonal vertical polarizations. Radar antenna scanned 360° sectors at elevation 0.5° with a pulse repetition time of 780 μs. The unambiguous range R_a and velocity v_a were 117 km and 35 m s^{-1} respectively. The number of samples for spectral analysis was 128. The thumbnails of plan position indicator (PPI) displays in Fig.1 shows the selected polarimetric variables: reflectivity in horizontal channel Z_h, velocity in horizontal channel v_h, differential reflectivity Z_{DR}, and backscatter differential phase δ. These variables are computed using standard processing technique (Doviak and Zrnic 1993) with no censoring. Only ranges up to 35 km (altitudes below 400 m) are shown. The ground clutter was removed in the frequency domain with an adaptive notch-and-interpolate filter. The fields of Z_h expose weak echoes in the earlier evening, which weaken further by 8 pm, and strengthen significantly by 9 pm. These are clear air echoes coming from different types of biological scatterers: a mix of diurnal birds and insects, insect alone, and a mix of nocturnal insects and migrating birds. The fields of v_h indicate moderate velocities increasing with the elevation and increasing at the later times. The fields of Z_{DR} expose values that reach 15 dB at 7:40 pm, and decrease to about 7 dB by 8 pm. Significant change at 8 pm is apparent. We attribute this change to the rapid replacement of the scattering content of the atmosphere triggered by sunset. We expect different scattering signature after sunset because the body shapes and sizes of the diurnal and nocturnal scatterers are not the same.

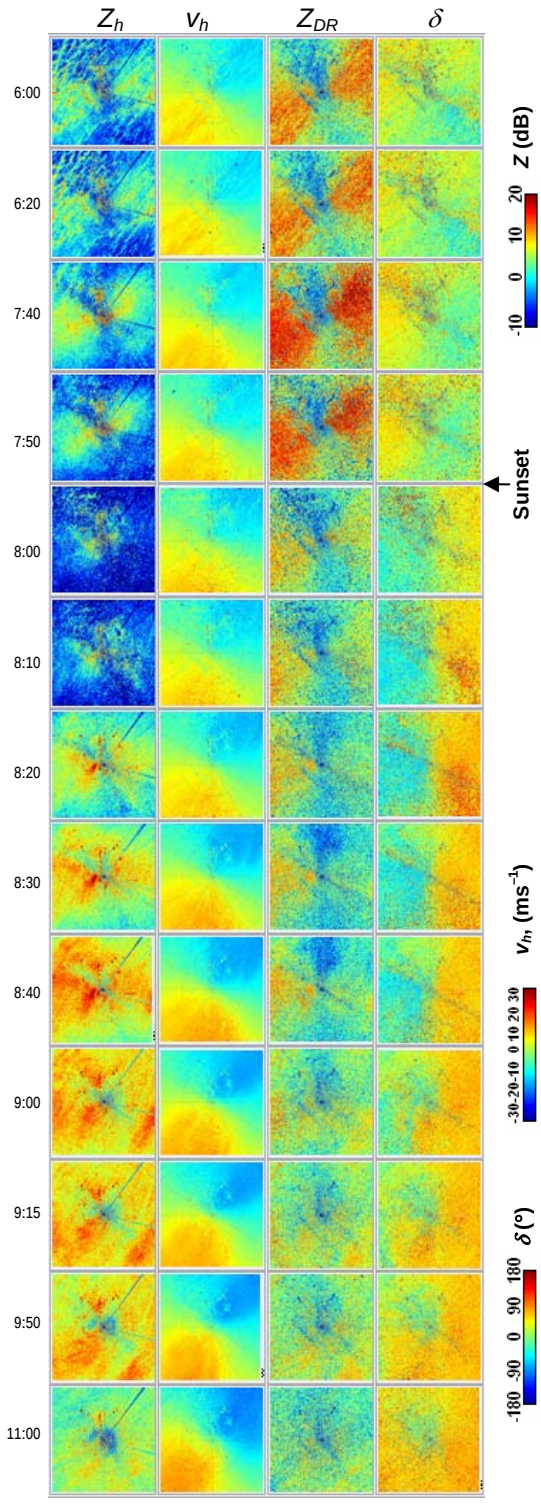

Fig.1. Thumbnails of PPIs zoomed to display up to 35 km in range. Columns (left to right) show Z_h, v_h, Z_{DR}, and δ at 0.5° elevation. Local times are indicated on vertical axes. Color scale for each variable is to the right. This case is occurred in clear air on Sept. 7, 2004.

3. POLARIMETRIC SPECTRAL ANALYSES

We estimate polarimetric spectral densities from the time-series weighted with the von Hann window. The spectral densities of Z_{DR} are computed for every H-V pair of spectral coefficients of the power spectral densities (Kezys et al. 1993, Yanovsky et al. 2005, Bachmann and Zrnic 2006). The spectral densities of complex co-polar correlation coefficient ρ_{hv} and backscatter differential phase δ are estimated as a magnitude and phase of a running 3-point average on the complex spectral coefficients (Bachmann and Zrnic 2006). The spectral densities of δ are corrected for the system phase, which is pre-estimated from the ground clutter reflectivity returns (Zrnic et al. 2005). With the sufficient number of pulses for spectral analyses, the polarimetric spectral densities can be used to discriminate contributions from scatterers with different Doppler velocities. Such situations occur if scatterers in the same resolution volume are moving with different radial velocities due to different headings or speeds. The presented data case has birds and insects mixed in different ratios at different times throughout the resolution volumes (Zhang 2006, Bachmann and Zrnic 2006). Example of polarimetric spectral densities that captures the signatures of birds and insects is shown in Fig.2. In this example, insects are dominant scatterers that stand out in the polarimetric spectral fields (Fig.2a-d). The spectral densities of power in horizontal channel S_h, differential reflectivity Z_{DR}, magnitude $|\rho_{hv}|$, and argument arg(ρ_{hv}) of complex co-polar correlation coefficient are computed for ranges from 30 to 35 km. We display these fields (Fig.2a-d) and plot the corresponding density values (Fig.2e-h) to emphasize the smoothness in the portions of the spectra contributed by insects' and noisiness contributed by other scatterers. The range averages expose the two-modal power spectrum and the one-modal polarimetric spectra (Fig.2i-l). The insects' contribution is distinct in all polarimetric spectra. Birds' contributions in this particular example are hidden in noise. If range averaging of polarimetric spectral densities is performed, the mean Z_{DR} and ρ_{hv} spectral densities of insects are higher than those of birds. In this paper we investigate signatures of scatterers producing polarimetric signatures with characteristic high Z_{DR} and high ρ_{hv} values. We have a high confidence that these scatterers are insects.

It is common for the spectral density of differential phase (Fig.2h) to have a noisy signature with a flat portion located at the velocities contributed by insects and weather. The mean of such spectra equals to the mean value at the corresponding range location of the field displayed on a PPI. Naturally, the averages obtained from such noisy signatures often result in the speckled field of the differential phase. We present a technique for estimating differential phase directly from the flat portion in spectral densities, avoiding contributions from the noisy portions.

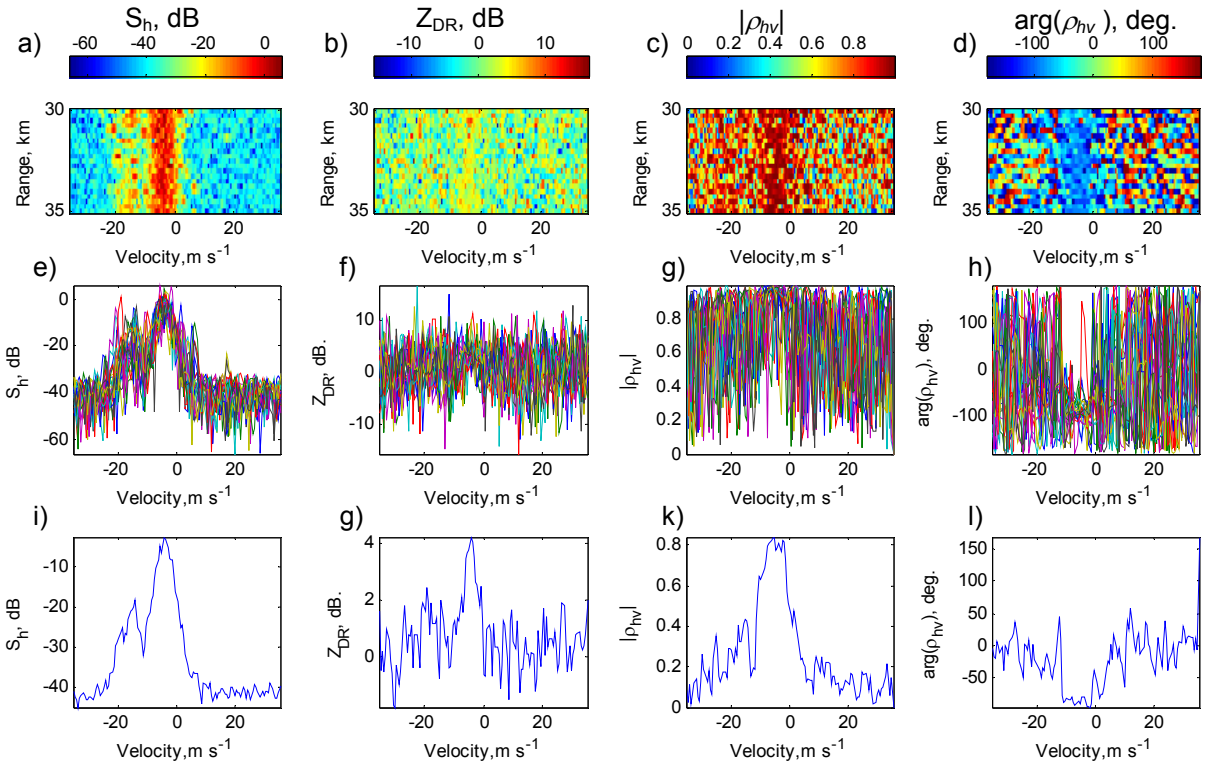

Fig.2. Example of polarimetric spectral densities along 5 km in a radial that contains signatures from insects and birds: (top) polarimetric spectral fields, (middle) polarimetric spectral fields plotted to expose spectral density values for reference; and (bottom) range averages of polarimetric spectral densities. This data are from 11 pm, 0.5° elevation, 160° azimuth, between 30 and 35 km range.

4. TECHNIQUE

In this section we present a technique for estimation of polarimetric variables only for the sections of spectral coefficients with high ρ_{hv} and high Z_{DR}.

1. Obtain the dual polarization time-series data along a radial at a certain azimuth.
2. Choose range interval for consideration (in our case, 5 km with 250 m range spacing resulted in two complex arrays [128×20] each).

For each range location

3. Use discrete Fourier transformation of the time series, optionally weighted by a window, to estimate complex spectral coefficients [128×1].
4. Estimate noise level at each range location: use complex spectral coefficients to obtain power spectral density; sort the spectral coefficients of the power spectral density in ascending order; select the quarter of spectral coefficients with smaller powers; average selected spectral coefficients to estimate the level of spectral floor/noise [1×1].
5. Filter ground clutter (we used and adaptive notch-and-interpolate filter on spectral coefficients near zero velocity if the power in these spectral coefficients exceeded the estimated noise level by 3 dB).
6. Compute spectral density of Z_{DR} from H-V pairs of spectral coefficients [128×1].
7. Estimate *complex-*ρ_{hv} spectral density for a 3-point running average on circular spectral coefficients [128×1].
8. Estimate phase of spectral coefficients obtained in step 7 and correct it for the system phase.
9. Estimate magnitude ρ_{hv} from spectral coefficients obtained in step 7.
10. Repeat steps 5–9 for all range locations in the radial.
11. Use the ρ_{hv} field [128×20] to obtain a $mask_1$ [128×1] by averaging in range.
12. Use the Z_{DR} field [128×20] to obtain $mask_2$ [128×1] by averaging in range.
13. Multiply normalized quantities from steps 11-12 ($mask = (mask_1/max(mask_1)) . \times (mask_2/max(mask_2))$) to obtain a vector [128×1] consisting of values between 0 and 1.
14. Use the value 0.5 as a threshold on the mask obtained in step 13.
15. Apply the mask from step 14 to the vectors obtained in steps 6, 8, and 9. Estimate the means values of polarimetric variables from the spectral coefficients within the unmasked window.
16. Repeat steps 1 – 15 for all azimuths

This technique extracts the signatures of scatterers with high ρ_{hv} and high Z_{DR} from spectra. The extracted signatures correspond to insects that are most likely weakly flying. Therefore, the spectral coefficients within the same window can be used for wind velocity computations. Next, we apply this procedure to evaluate insects' polarimetric signatures between ranges 30 and 35 km and at different times of the evening.

5. EXAMPLES

5.1. Polarimetric variables of insects within the range interval 30 and 35 km and their interpretation

The polarimetric variables computed using presented adaptive technique are in Fig.3a-c. These examples depict the change of insects' intrinsic polarimetric variables in time and azimuth. The uneven spacing in collection of volume scans causes empty columns in the images. The discontinuities that appear as paths at about 120° and 300° are due to a partial degradation of signals from ground clutter filtering in the region of zero radial velocity of wind. Overall images show that a big change happened at 8 pm immediately after the sunset. The differential phases for the 7:50 pm and the 8 pm times are in Fig.3d-e. The "flip" in phases prompted by sunset is evident in Fig.3a. The peak values of Z_{DR} are reaching 10 dB at 6 pm, increase to 12 dB at 7 pm and decrease to 5 dB to the east and 7 dB to the west of the radar by 8 pm. Before the sunset, Z_{DR} is two-modal with about 12 dB maxima and indicating symmetric body shapes; ρ_{hv} is one-modal and low between 0.75 and 0.9, indicating large bodies and/or more chaotic movements; δ is one-modal with high values to the west and low values to the east. After the sunset, Z_{DR} is one-modal with about 7 dB maximum; ρ_{hv} is slightly higher; δ is one-modal with high values to the east and low values to the west. Before the sunset, the insects are diurnal, large and likely have with simple prolate body shapes. An increase in Z_{DR} from 6 pm to 7:50 pm might be caused by the change in orientation during descent. At the dusk the insects' body shapes and orientation exhibit signatures that defy simplistic explanations.

5.2. *Backscatter differential phase of insects*

The backscatter differential phase of insects computed using the presented adaptive technique is shown in Fig.4a-e. The ranges are from 20 km to 45 km, corresponding to beam height of 200 m to 500 m. The fields of backscatter differential phase are very smooth and show similar values at different ranges/altitudes. The similarity of the fields indicate that the extracted type of insects were present throughout the chosen area. The flip in the differential phase is evident in all images Fig.4a-e. The phase flip is an important observation that we are attempting to understand. A continuous sunset-data and detailed

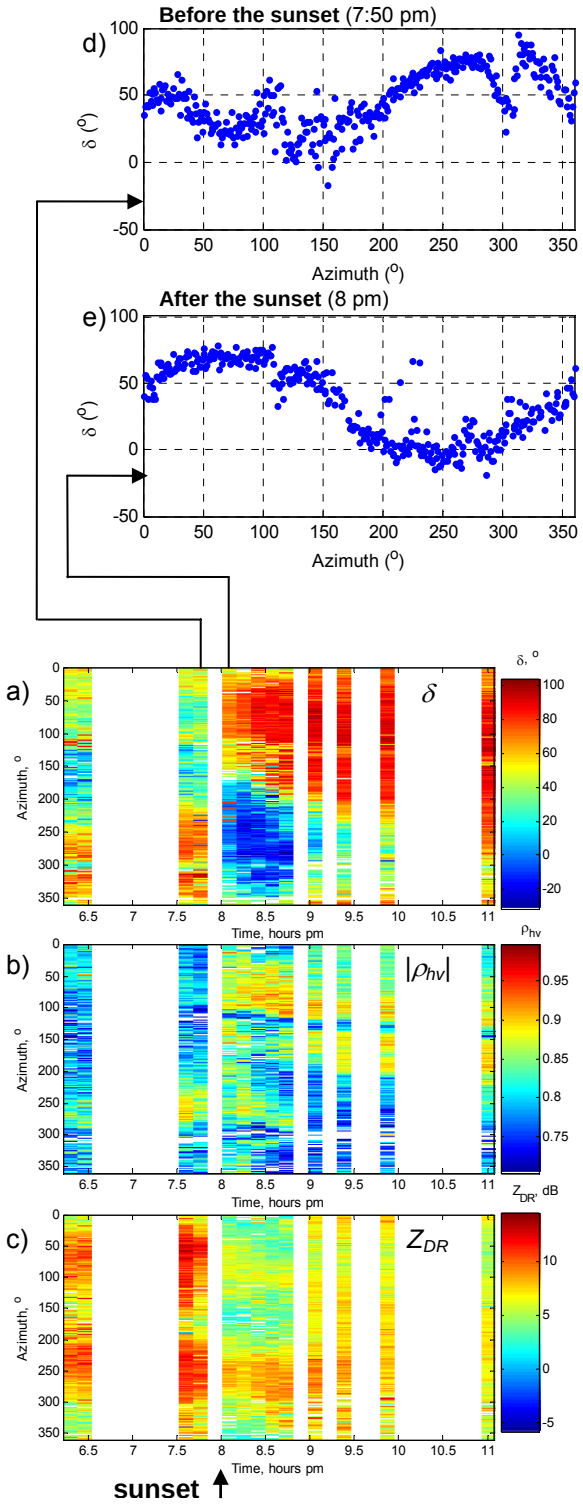

Fig.3. Polarimetric variables extracted from spectra of insects: (a) δ, (b) ρ_{hv}, and (c) Z_{DR}. These data are from 0.5° elevation, and ranges between 30 and 35 km.

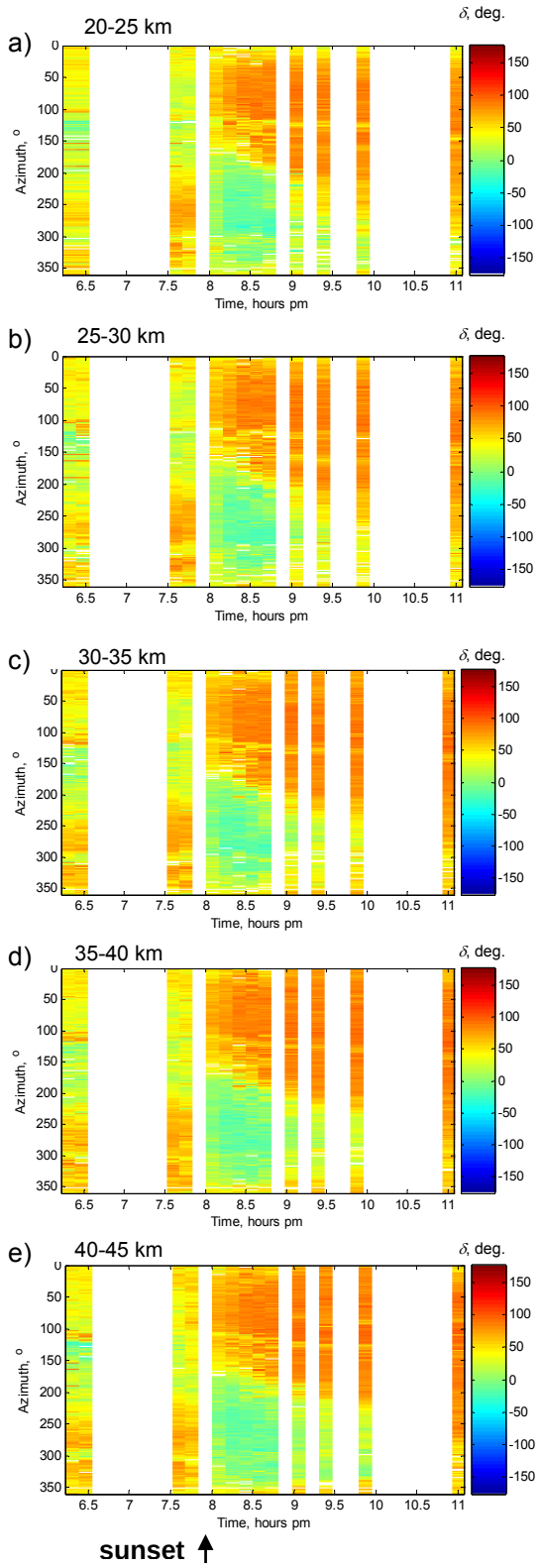

Fig.4. Backscatter differential phase inherent to insects at 0.5° elevation, and 5 km in range starting at a) 20 km, b)25 km, c) 30 km, d) 35 km, and e) 40 km.

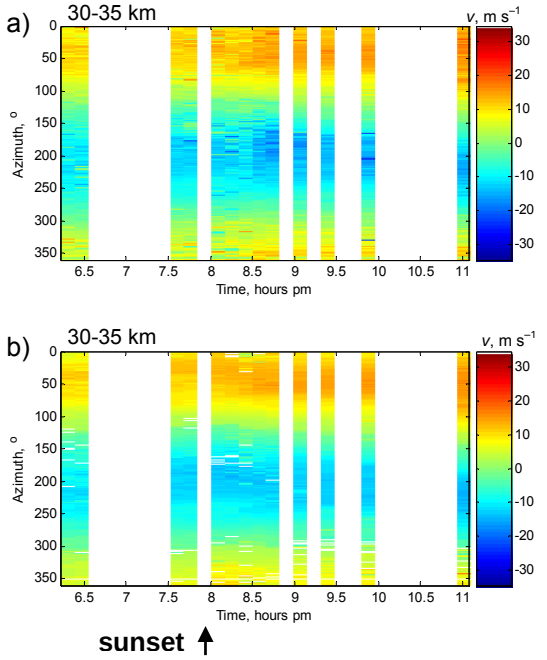

Fig.5. Mean velocity for 5-km range interval between 30 and 35 km at 0.5° elevation computed for (a) all contributors to the spectrum; (b) only insects contributions.

Study might help to explain the flip in phases during the sunset. We speculate that there could be several types of diurnal insects. One kind of diurnal insect is fast. It orients downward for the descent before the sunset, descends rapidly, and has mostly landed by the dusk. The other kind of diurnal insect is slow. It starts descending long before the sunset, continues slow descend through the dusk and into the late evening. Fig.4. depicts negative values of δ from 8 pm to about 9:30 pm and between 200° and 330° azimuths, supporting the slow-descend hypothesis. Another hypothesis is that one type of nocturnal insects ascended immediately after the sunset (8 pm to 9 pm) but was gradually replaced by different nocturnal insects (11 pm). Note the reflectivity fields (Fig.1) indicate smaller powers at 11 pm compared to 9:50. Thus there could be diurnal, nocturnal, and transitional types of insects all with a characteristic signature of backscatter differential phase. Observed diurnal insects produce δ-signature that is symmetric and resembles a sinusoid (Fig.3d). The transitional type of insects is up from 8 to 10 pm and also has a symmetric δ-signature but with different polarity (Fig.3e). Observed nocturnal insects have a flat δ-signature with values near 80°.

The Doppler velocity estimated for all contributors to the spectra and for extracted insects contributions are presented in Fig.5a-b. These are averages over 5 km in range between 30 and 35 km. Larger velocity values up to 20 m/s in Fig.5a and late in the evening are due to averaging contribution from birds and

insects. Fig.5b depicts smother fields with velocities below 15 ms throughout the evening.

6. CONCLUSIONS

We presented an approach for estimating intrinsic polarimetric variables of insects. The polarimetric signatures are analyzed in the frequency domain and an adaptive mask is created to suppress contributions from non-insect scatterers. Presented approach extracts signatures of the type of insects that can be characterized by high values of differential reflectivity and high values of co-polar correlation coefficient. We used backscatter differential phase inherent to insects to observe changes in insects backscatter signatures (averaged 5-km in range) over the evening. The insects' signatures indicate complicated body shapes which can not be described with simple spheroid body model. We documented an abrupt change (flip) in the backscatter differential phases during the sunset. We attribute this flip to the change of occupants of the atmosphere from diurnal to nocturnal biological scatterers.

The wind signature can be estimated from adaptively selected (based on backscatter differential phase and differential reflectivity) spectral coefficients. The wind parameters can be estimated directly from the insects' signatures even in the presence of migrating birds. The presented automated procedure can be used to compute intrinsic polarimetric variables of other types of scatterers if the selection parameters are modified. Moreover, our procedure could be adopted to estimate intrinsic polarimetric variables in storms.

Acknowledgements

For the first author funding was provided by NOAA/Office of Oceanic and Atmospheric Research under NOAA-University of Oklahoma Cooperative Agreement #NA17RJ1227, U.S. Department of Commerce.

8. REFERENCE

Bachmann S. M., and D. S. Zrnić, 2006: Spectral Density of polarimetric variables separates biological scatterers in the VAD display. *Jour. Atmos. Oceanic Technology*, in print.

Doviak R. J., and D. S. Zrnić, 1984: *Doppler Radar and Weather Observations*. Academic Press, 458 pp.

Kezys V., E. Torlaschi, and S. Haykin, 1993: Potential capabilities of coherent dual polarization X-band radar. Preprints, 26th Int. Conf. on Radar Meteorology, Norman, OK, Amer. Meteor. Soc., 106-108.

Yanovsky, F.J., H.W.J. Russchenberg, and C.M.H. Unal, 2005: Retrieval of information about turbulence in rain by using Doppler-polarimetric Radar. *IEEE Trans. Microw. Theory Tech.*, **53,** 444-450.

Zrnić D. S, and A. V. Ryzhkov, 1998: Observation of Insects and Birds with Polarimetric Radar. *IEEE Trans. Geosci. Remote Sens.*, **36**, 661-668.

Zrnić D. S., V. M. Melnikov, and A.V. Ryzhkov, 2005: Correlation coefficients between horizontally and vertically polarized returns from ground clutter. *Jour. Atmos. Oceanic Technology*, **23**, 381-394.